

New amorphous oxides as high capacity negative electrodes for lithium batteries: the Li_xMVO_4 ($\text{M} = \text{Ni}, \text{Co}, \text{Cd}, \text{Zn}; 1 < x \leq 8$) series

D. Guyomard, C. Sigala, A. Le Gal La Salle, Y. Piffard

Laboratoire de Chimie des Solides, Institut des Matériaux de Nantes, 2 rue de la Houssinière, 44072 Nantes Cedex 03, France

Accepted 28 October 1996

Abstract

The crystallized precursors LiMVO_4 ($\text{M} = \text{Co}, \text{Ni}, \text{Cd}, \text{Zn}$) are irreversibly transformed to lithiated amorphous oxides Li_xMVO_4 (x close to 8) during the first Li insertion in a lithium battery. Under low rate, these amorphous oxides cycle large amounts of Li per formula unit in the 0.02–3 V range (versus Li), with an average voltage in the order of 0.6 V for Li insertion and 1.4 V for Li extraction. In the case of Li_xNiVO_4 at first Li extraction, for example, $\Delta x = 6.6$ and $Q = 980$ Ah/kg (active material alone) or 900 Ah/kg (calculated with respect to the total mass: material + carbon black) or 4230 Ah/l (active material alone), more than 5.5 times the volumic capacity of graphite. The cycling behavior at fast rate ($C/6$) was very good with a peculiar increase in capacity with cycle number after an initial decrease. Characterization of lithiated Li_xNiVO_4 samples, performed with the use of local techniques such as X-ray absorption spectra (XAS) and electron energy loss spectroscopy (EELS), led to an evaluation of the average oxidation states of V and Ni and of the electronic transfer from Li to V and Ni. Results are compatible with the crystal chemistry of Ni and V oxides. The Li ‘incorporation/extraction’ process in the series Li_xMVO_4 is not a destruction/reconstruction mechanism involving Li_2O and M and V metals. However, it seems to be different from a classical topotactic intercalation reaction. © 1997 Published by Elsevier Science S.A.

Keywords: Lithium batteries; Amorphous oxides; Negative electrodes

1. Introduction

Research for new negative electrode materials has been strongly stimulated by the recent development of lithium-ion batteries [1]. Such materials are expected to deliver a large reversible capacity at low voltage versus Li, with a weak capacity loss during the first cycle and a good cycleability over several hundreds of cycles.

It is quite difficult to obtain these three main parameters with both favorable values in the same material. Very high capacity (600 to 900 Ah/kg) negative electrode materials with low voltage (≤ 0.5 V versus Li) are mainly carbonaceous compounds (nongraphitizable hard carbons and hydrogen-containing carbons [2]) and multi-metallic alloys [3], but generally the carbonaceous compounds show a large capacity loss during first cycle while the multi-metallic alloys suffer from low cycleability. Other compounds prepared in the lithiated form, such as nitrides ($\text{Li}_{3-x}\text{M}_x\text{N}$ with $\text{M} = \text{Co}, \text{Ni}, \text{Cu}$ [4]) offer good performance, but are air-sensitive. Finally graphites, which exhibit a reversible capacity close to 400 Ah/kg at about 0.15 V versus Li with a 7% initial capacity loss [5], still seem to allow the best compromise.

Oxides, such as WO_2 [6–8], MoO_2 [8], TiO_2 [9], $\text{Li}_4\text{Ti}_5\text{O}_{12}$ [10], Nb_2O_5 [11] and $\text{Li}_6\text{Fe}_2\text{O}_3$ [12–14] generally lead to weak capacities (< 200 Ah/kg) and average voltages in the 1.0–1.6 V range (versus Li) for oxidized starting compounds (W, Mo, Ti and Nb oxides), or close to 0.1 V versus Li for reduced starting compounds ($\text{Li}_6\text{Fe}_2\text{O}_3$).

Fuji Photo Film reported recently (April 1996) on a new generation of non-carbon high capacity and safe Li-ion batteries, using SnO_2 -based oxides with 400–500 Ah/kg capacity and about 0.4 V average voltage (versus Li) as the negative electrode [15]. This paper deals with another family of amorphous transition metal oxides that can be also used as high capacity negative electrode materials [16,17]. Their synthesis, an investigation of their electrochemical properties and the characterization of intercalated materials are reported herein.

2. Experimental

LiMVO_4 ($\text{M} = \text{Co}, \text{Ni}, \text{Zn}, \text{Cd}$) crystallized precursors were prepared by solid state reaction at 500 °C under air [17]. Co and Ni compounds adopt the spinel structure whereas

LiCdVO_4 and LiZnVO_4 exhibit a pseudo-olivine and the phenacite structure, respectively. A common feature to all these structures is the presence of vanadium (V) in the tetrahedral structure. The theoretical density of these materials is 4.23, 4.32, 3.38 and 4.43 for $M = \text{Co}, \text{Ni}, \text{Zn}$ and Cd , respectively.

Electrodes were made by mixing the active materials with carbon black and an organic binder polyvinylidene fluoride (PVDF). The mixture was deposited [5] onto a stainless-steel disk current collector. The mass composition of the composite electrodes was (86:9:5) (active material:carbon black:binder) for low-rate experiments (cyclic voltammetry). The carbon black content of the composite electrodes was increased (up to 30% in some electrodes) for fast-rate cycling experiments.

Such made composite materials were used as the positive electrode in test cells with the chain: Li/ethylene carbonate + dimethyl carbonate (1:2) + 1 M LiClO_4 /electrode. Then, a discharge corresponds to Li insertion and a charge to Li extraction. The cells were tested using the 'Mac-Pile' system (Biologic, Claix, France) in galvanostatic and potentiodynamic modes. If not specified, reported specific capacities are calculated with respect to the total mass (active material + carbon black) and voltages are reported versus Li/Li⁺ system.

X-ray absorption spectra (XAS) were collected in transmission mode at the V and Mn *k*-edges at LURE (Laboratoire d'utilisation du rayonnement électromagnétique, Orsay, France) on the DCI ring. The EELS (electron energy loss spectroscopy) images were recorded in the diffraction coupling mode with the use of a GATAN 666 parallel spectrometer on a Philips CM30 microscope running at 150 kV. Details concerning data acquisition and analysis will be found in Ref. [18] for XAS and in Ref. [19] for EELS.

3. Results

3.1. Comparative Li insertion behavior

Lithium insertion in LiMVO_4 crystallized precursor materials was investigated in a potentiodynamic mode at a slow scan rate. The current–voltage behavior obtained over the first discharge/charge cycles with LiCoVO_4 , as an example, is reported in Fig. 1. The first discharge (insertion of lithium) is different from the following ones which are identical to each others. It corresponds to an irreversible transformation of the precursor leading to an amorphous lithiated new material (as determined from its X-ray diffractogram (XRD)), that further de-intercalates and re-intercalates Li with almost no evolution from one cycle to the other. In the following, precursors and amorphous oxides will be denoted as LiMVO_4 and Li_xMVO_4 , respectively, to avoid any confusion.

This current–voltage behavior corresponds in fact to Li insertion in both the active material and the carbon black (mixed with the material to prepare the electrode). After subtraction of the latter contribution [20] (it corresponded to less than 4% of the total capacity) according to a method described in Ref. [21], the *I*-*V* curves were integrated and the intrinsic capacity of the materials was expressed as the Li composition per formula unit. Such *V*-*x* curves obtained for the different materials in the optimized voltage range are compared in Fig. 2. According to the nature of M, either 1 or 2 or 4 electrochemical processes are observed for Li_xMVO_4 materials (after the first discharge) in the whole voltage range, with quite a large polarization. A striking result is the very large Li composition in all materials (about Li_8MVO_4) at the end of discharge and the large amount of Li reversibly extracted during the charge (5 to 6 Li per formula unit).

The main parameters characterizing the materials as the negative electrode of an Li battery were determined from

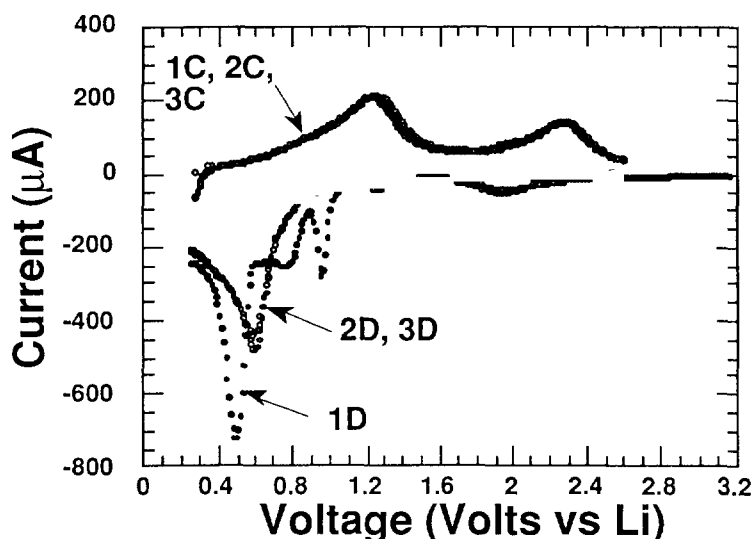


Fig. 1 Current vs. voltage curves obtained for LiCoVO_4 composite electrodes at the three first cycles, measured by cyclic voltammetry at 50 mV/h between 0.25 and 2.6 V. The *n*th discharge and charge are respectively denoted *n*D and *n*C

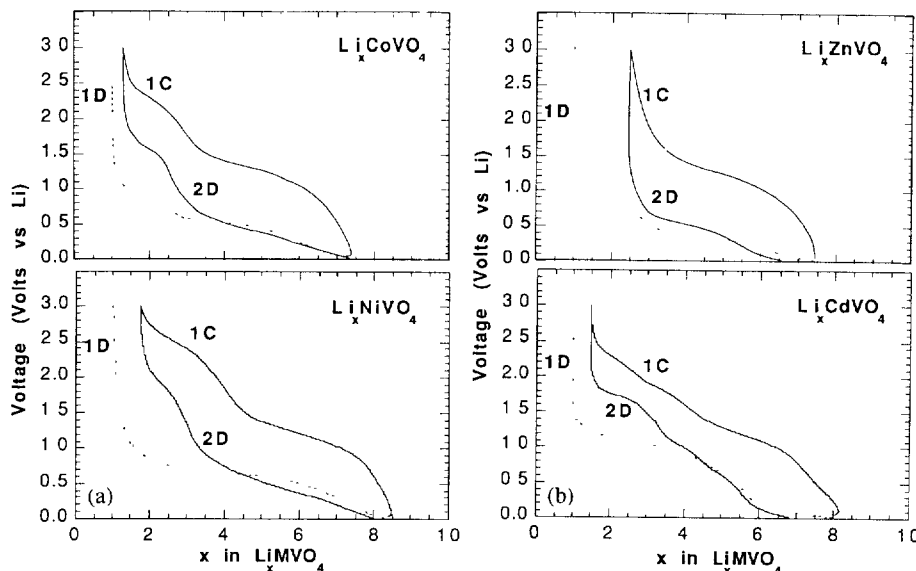


Fig. 2 (a), (b) Voltage vs. Li composition curves, intrinsic to Li_xMVO_4 materials, at the three first half-cycles, measured by cyclic voltammetry at 10 mV/h between 0.02 and 3 V. The n th discharge and charge are respectively denoted nD and nC .

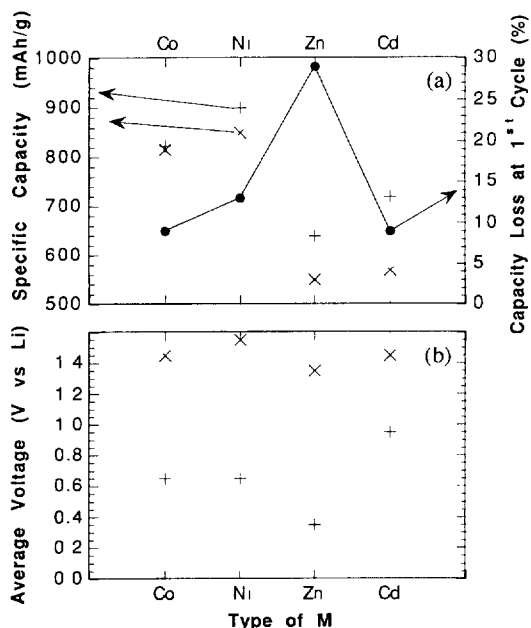


Fig. 3 Dependence of the reversible specific capacity (calculated with respect to the total mass: active material + carbon black). Fig. 3(a) (at first charge (+) and second discharge: (x)), the capacity loss at first cycle (Fig. 3(a) (●)) and the average Li insertion (Fig. 3(b)) (+) and extraction (Fig. 3(b)): (x) voltages on the nature of M in Li_xMVO_4 . Note that the capacity loss at first cycle was calculated from the comparison of the first discharge of the precursor compound and the first charge of the amorphous oxide prepared in situ during the first discharge.

previous experiments; they are summarized in Fig. 3. The performance vary slightly with M: Co; Cd-based compounds show the lowest initial capacity loss, LiNiVO_4 gives the largest capacity and LiZnVO_4 delivers the lowest voltage. Very large reversible specific capacities are obtained indeed, larger than 800 Ah/kg for LiMVO_4 ($M = \text{Co}, \text{Ni}$), more than twice that of graphite. It corresponds to volumic capacities larger

than 3500 Ah/l (per liter of active material alone), 4.7 times that of graphite.

3.2. Cycling behavior

Previous experiments correspond to very slow cycling rates. The cycleability over more than 100 cycles was then tested in galvanostatic mode and under more rapid conditions (cycling rate greater than $C/10$), compatible with application. For such experiments, the carbon black content of the composite electrodes was increased in order to enhance the electronic conductivity of the electrodes.

Some parameters were found to have a drastic influence on the cycleability of the electrodes. Fig. 4 compares the only influence of first discharge rate on further cycling behavior. A first discharge at a very low rate leads to the best result. These data show (i) that the irreversible transformation of the precursor has a slow kinetics and then needs time (several

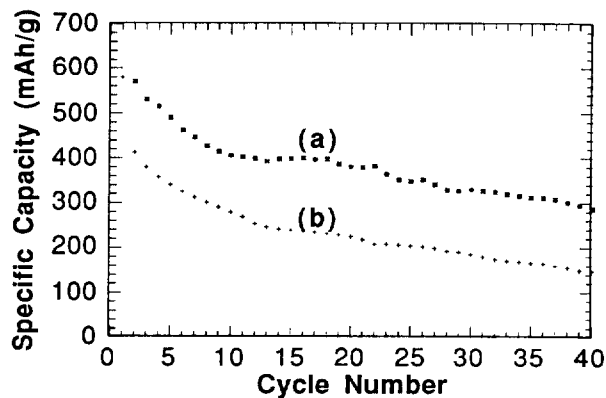


Fig. 4. Influence of the first discharge rate on the further cycleability of a Li_xCoVO_4 composite electrode (mass ratio = (79:16.5)), cycled at a rate corresponding to 1 Li per LiCoVO_4 per h, between 0.02 and 2.6 V. The first discharge rate was either (a) $C/100$ or (b) $C/15$.

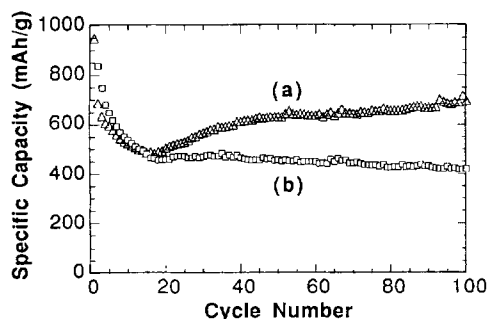


Fig. 5 Influence of an in situ electrochemical treatment (see text) (a) after treatment or (b) without treatment on the further cycleability of an Li_xZnVO_4 composite electrode (mass ratio = 1.65.30:5), cycled at a rate corresponding to 1 Li per LiZnVO_4 per h, between 0.02 and 3.9 V, after a first discharge at $C/60$ rate.

tens of hours) to be completed, and (ii) that a deeply transformed amorphous oxide cycles better.

An in situ electrochemical treatment, consisting of 20 discharge/charge cycles in the 2.4–3.9 V range in which only a negligible capacity is obtained, was applied after the end of first charge. Data obtained with LiZnVO_4 are shown in Fig. 5. That specific treatment leads to a spectacular improvement in cycleability, with a capacity that increases after several tens of cycles, instead of remaining at a constant level. The reason for such a result is not clear; it could come from a kind of electrochemical grinding of the material particles, leading to further smaller grains that present a more favorable overall kinetics [22]. The same kind of results was observed with other Li_xMVO_4 materials. The effect of such an in situ electrochemical treatment on the cycling behavior of the electrodes should also be tested in the case of other oxide and non-oxide materials, including positive electrode materials.

The cycling behavior of the electrodes, tested between 0.02 and 3.9 V over more than hundred cycles at a cycling rate close to $C/6$ is compared in Fig. 6. No optimization of the particle size or morphology was applied to get such a behavior. The capacity decreases over the first 10 to 100 cycles and then increases for those electrodes that were subjected to the above electrochemical treatment. The Zn- and Ni-based com-

pounds still deliver capacities greater than 600 Ah/kg after 150 cycles.

3.3. Characterization of lithiated oxides

Amorphous Li_xMVO_4 oxides are lithiated up to about 8 Li per formula unit. The existence of such large Li compositions and the possibility to reversibly extract Li from these samples raises important basic questions dealing with structural aspects and electronic transfer. To get answers, samples with different lithium contents were prepared electrochemically and characterized using local techniques such as XAS and EELS.

The nickel k -edge XANES (X-ray absorption near edge spectroscopy) images and $L_{2,3}$ EELS spectra of the different samples were very similar and then did not allow any evaluation of the Ni oxidation state and local environment as a function of the Li content. It seems very qualitatively that Ni was almost not affected by the electrochemical processes.

On the contrary, the vanadium k -edge XANES spectra were very dependent on the Li content. The XANES spectra at vanadium k -edge of Li_xNiVO_4 samples with different Li contents are shown in Fig. 7. The pre-edge peak (5470 eV) intensity drastically decreases as soon as the first Li (per formula unit) is intercalated in the material, showing that the vanadium site is no longer tetrahedral. This is very likely a consequence of a vanadium reduction. This reduction proceeds when x increases, as indicated by the shift to lower energies of the absorption edge (in the 5475–5485 eV range). Simultaneously, the pre-edge peak intensity varies. It remains much weaker than for the starting compound but not negligible, thus indicating that the vanadium site is likely octahedral, but rather distorted. Consequently, an evaluation of the vanadium average oxidation state (AOS) from the edge position would not be very accurate.

Qualitative comparison of spectra measured on samples obtained after different electrochemical treatments clearly shows that the initial compound is not restored after one discharge/charge cycle, but that one and a half cycle (dis-

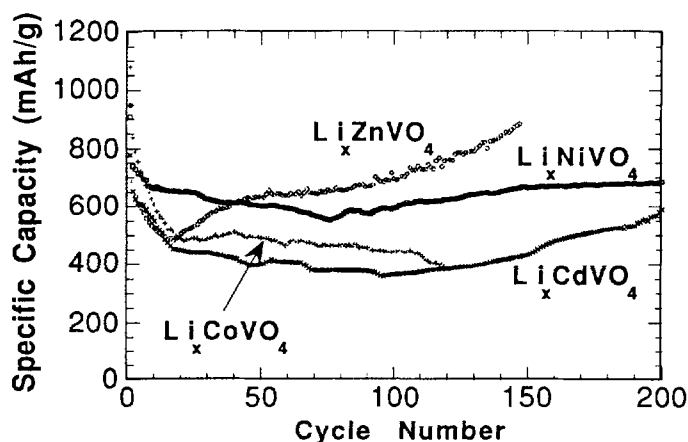


Fig. 6. Cycling behavior of Li_xMVO_4 composite electrodes at about $C/6$ between 0.02 and 3.9 V vs. Li. An electrochemical treatment (see text) was applied to all materials except to Li_xCoVO_4 .

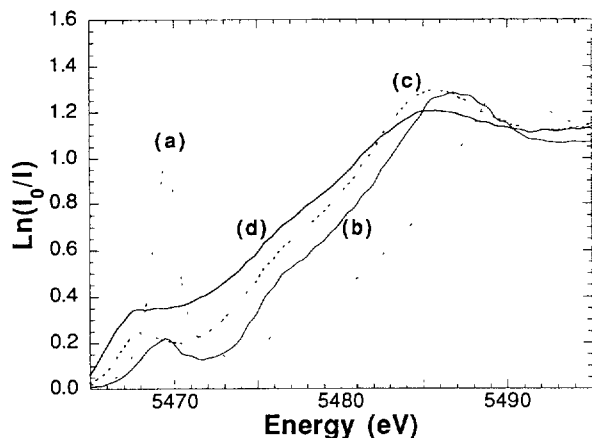


Fig. 7. Comparison of the vanadium k -edge XANES spectra of (a) LiNiVO_4 and (b) Li_xNiVO_4 compounds electrochemically prepared during the first discharge, with: (b) $x = 3$, $x = 5.5$, and $x = 8$

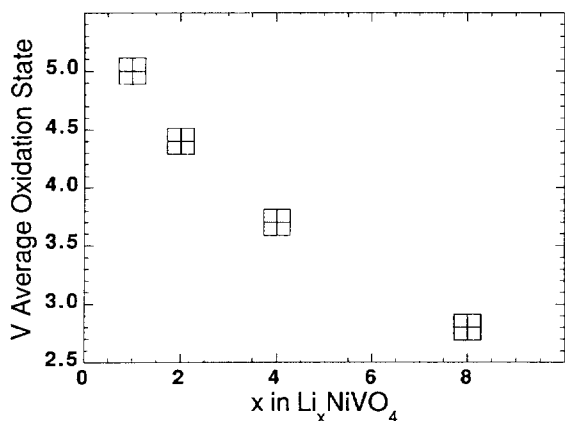


Fig. 8. Variation of the vanadium average oxidation state with Li content in Li_xNiVO_4 .

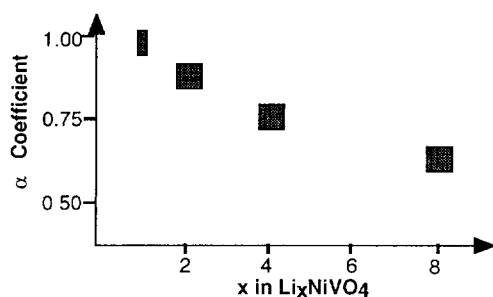


Fig. 9. Evolution of the α coefficient (see text) with Li content in Li_xNiVO_4

charge/charge/discharge) leads to the same material as after the first discharge. This result is in accordance with XRD and electrochemical data, that demonstrated an irreversible transformation of the precursors during the first discharge and further cycleability of amorphous oxides.

EELS spectra were recorded for lithiated oxides. The energy position of the vanadium l_3 edge was used to determine the vanadium AOS, by comparison with standards [23]. The results, reported in Fig. 8, show an important reduction of vanadium cations upon Li insertion. However, the AOS remains higher than expected from the number of Li inserted per formula unit.

Li k -edge EELS spectra show that the position of the edge depends on the Li content of the material. A correlation between the edge energy and the ionisation state of Li has already been demonstrated in some compounds [24]. On account of this, the α coefficient describing the electronic transfer from Li to the host matrix was determined from a direct measurement of the Li k -edge energy. An arbitrary linear scale was used, taking α as equal to 0 and 1 for the energy measured with Li metal and Li_2S , respectively. Fig. 9 shows a continuous decrease of α versus x which indicates that the electronic transfer from Li to the host matrix decreases with increasing x in Li_xNiVO_4 .

4. Discussion of the insertion mechanism

A major question is to know if the Li incorporation mechanism corresponds to a destruction of the initial structure leading to Li_2O and M and V metals, as was demonstrated for $\text{Li}_6\text{Fe}_2\text{O}_3$ [25]. The same mechanism was also observed for many chalcogenides: (γ - Li_xMX_2 'phases' (M = Mo, W; X = S, Se or Te; $x > 1$)) contain in fact mixtures of Li_2X and metallic M [26]). In such a case, partial Li extraction from lithiated samples was observed and interpreted as a partial reconstruction of the initial structure by diffusion of the metal back into the oxygen network [25].

Data presented in this paper clearly show that Li 'incorporation/extraction' process in the series Li_xMVO_4 is not a destruction/reconstruction mechanism for the following reasons:

(i) Electrochemical data obtained at very low rate do not present a plateau during the charge, corresponding to the Gibbs free energy formation of Li_2O , as was the case for Li_2X (X = S, Se, Te) in chalcogenides [26]. Moreover, fast cycling rates (1 Li per LiMVO_4 every 1 h) lead to very large capacities (6 Li per LiMVO_4) over several hundreds of cycles.

(ii) XRDs were characterized by an amorphous compound and did not show broad lines corresponding to Li_2O , as was the case for Li_2X in chalcogenides [26].

(iii) XAS and EELS data indicate the absence of Ni and/or V metals in the lithiated compounds. All particules analyzed by EELS were homogeneous.

The large reversible capacity values measured for Li_xMVO_4 amorphous oxides correspond to large differences in Li compositions, such as $\Delta x > 6.5$. Such large values were never reported for oxides in the literature up to now. The Li 'incorporation/extraction' process in the series Li_xMVO_4 is then believed to be different from a classical topotactic intercalation reaction. Further studies are needed to understand such a mechanism.

5. Conclusions

The Li_xMVO_4 (M = Co, Ni, Cd, Zn) amorphous oxides were prepared by a two-step process: (i) solid-state synthesis

of LiMVO_4 crystallized precursors at 500 °C in air, (ii) followed by an electrochemical lithiation in a lithium battery. They contain about 8 Li per formula unit and de-intercalate reversibly between 70 and 90% of the inserted Li (as a function of M) over several charge/discharge cycles.

Cycling capability was tested under fast rate (faster than C/10) compatible with application purpose. Capacities larger than 600 Ah/kg (calculated with respect to the total mass: active material + carbon black), over more than 100 cycles, were achieved with Zn- and Ni-based materials.

Ex situ XAS and EELS studies, at V and Ni absorption edge of lithiated samples, indicated that vanadium AOS regularly decreases down to about 2.6 and that Ni average oxidation state remains close to 2, when Li was inserted in LiNiVO_4 materials up to 8 Li per formula unit. Such AOS values are reasonable, in accordance with the crystal chemistry of Ni and V oxides. Energy of Li *k*-edge electron absorption allowed to determine the α coefficient describing the electronic transfer from Li to the host matrix: results show a decrease in charge transfer when the Li content increases, compatible with the AOS, still quite high, of transition elements in lithiated compounds.

The amorphous oxides with the formulation Li_xMVO_4 ($1 < x \leq 8$ and M = Co, Ni, Cd, Zn) seem to be a new category of intercalation compounds with a very high capacity at low voltage. They could be interesting candidates as the negative electrodes in very high capacity Li-ion batteries delivering a lower output voltage than carbon-based batteries.

References

- [1] J.M. Tarascon (ed.), Rechargeable lithium batteries, *Solid State Ionics*, 69 (1994) 201–308.
- [2] J.R. Dahn, T. Zheng, Y. Liu and J.S. Xue, *Science*, 270 (1995) 570.
- [3] J. Yang, M. Winter and J.O. Besenhard, *Ext. Abstr., 10th Int. Conf. Solid State Ionics, Singapore, 3–8 Dec 1995*, p. 288.
- [4] T. Shodai, S. Okada, S.I. Tobishima and J.I. Yamaki, *Ext. Abstr., 10th Int. Conf. Solid State Ionics, Singapore, 3–8 Dec 1995*, p. 193.
- [5] D. Guyomard and J.M. Tarascon, *Solid State Ionics*, 69 (1994) 222.
- [6] B. Di Pietro, M. Patriarca and B. Scrosati, *Synth. Met.*, 5 (1982) 1.
- [7] J.J. Auborn and Y.L. Barberio, *J. Electrochem. Soc.*, 134 (1987) 638.
- [8] K.M. Abraham, D.M. Pasquariello, E.B. Willstaed and G.F. McAndrews, in J.P. Gabano, Z. Takehara and B. Bro (eds.), *Proc. Symp. Primary and Secondary Ambient Temperature Lithium Batteries, 1988*, The Electrochemical Society, Proc. Vol. 88-6, Pennington, NJ, USA, 1988, p. 668.
- [9] S.Y. Huang, L. Kavan, I. Exnar and M. Gratzel, *J. Electrochem. Soc.*, 142 (1995) L142.
- [10] T. Ohzuku and A. Ueda, *Solid State Ionics*, 69 (1994) 201.
- [11] N. Kumagai, I. Ishiyama and K. Tanno, *J. Power Sources*, 20 (1987) 193.
- [12] S. Morzilli, B. Scrosati and F. Sgarlata, *Electrochim. Acta*, 30 (1985) 1271.
- [13] M.M. Thackeray, W.I.F. David and J.B. Goodenough, *Mater. Res. Bull.*, 17 (1982) 785.
- [14] K.M. Abraham, D.M. Pasquariello and E.B. Willstaed, *J. Electrochem. Soc.*, 137 (1990) 743.
- [15] I. Yoshio, M. Masayuki, M. Yukio, K. Tadahiko and M. Tsutomu, *Eur. Patent No. 0 651 450 A1* (21 Oct. 1994).
- [16] I. Yoshio, *Eur. Patent No. 0 567 149 A1* (23 Apr. 1993).
- [17] C. Sigala, D. Guyomard, Y. Piffard and M. Tournoux, *CR Acad. Sci. Paris*, 320 (IIb) (1995) 523.
- [18] B.K. Teo, *EXAFS, Basic Principles and Data Analysis*, Springer, Berlin, 1986.
- [19] J.L. Mansot, P. Leone, P. Euzen and P. Palvadeau, *Microsc. Microanal. Microstruct.*, 5 (1994) 79.
- [20] C. Sigala, A. Le Gal La Salle, D. Guyomard and Y. Piffard, *J. Electrochem. Soc.*, submitted for publication.
- [21] D. Guyomard and J.M. Tarascon, *J. Electrochem. Soc.*, 140 (1993) 3071.
- [22] J.M. Tarascon, personal communication.
- [23] W.G. Waddington, P. Rez, J.P. Grant and C.J. Humphreys, *Phys. Rev. B*, 34 (1986) 1467.
- [24] J.L. Mansot, C. Auriel, J. Wery and A. Meershaut, *Proc. SFME Conf., Lyon, France, 1993*.
- [25] M.M. Thackeray, W.I.F. David and J.B. Goodenough, *J. Solid State Chem.*, 55 (1984) 280.
- [26] L.S. Selwyn, W.R. McKinnon, U. Von Sacken and C.A. Jones, *Solid State Ionics*, 22 (1987) 337.